

Automatic Mode Switching of P/PI Speed Control for Industry Servo Drives Using Online Spectrum Analysis of Torque Command

Jul-Ki Seok, *Member, IEEE*, Kyung-Tae Kim, and Dong-Choon Lee, *Member, IEEE*

Abstract—Conventional proportional/proportional–integral (P/PI) speed controller for today’s servo drives has to be manually tuned at the controller switching set point by trial and error, which may translate into drive system downtime and a subsequent loss of productivity. The adjustable drive performance is heavily dependent on the quality of expert knowledge. The performance becomes inadequate in applications where the operating conditions change in a wide range, i.e., tracking command, acceleration/deceleration time, and load disturbances. In this paper, we discuss the demands on simple controls/setups for industry servo drives. Analyzing the frequency content of the motor torque command, P/PI speed control mode switching is automatically performed with only a prior knowledge of the mechanical time constant. The dynamic performance of the proposed scheme assures a desired tracking response curve with minimal oscillation and settling time over the entire set of operating conditions. For a comprehensive comparison of conventional P/PI control scheme, we carried out extensive tests on an actual servo system.

Index Terms—Frequency content of motor torque, industry servo drive, proportional/proportional–integral (P/PI) speed controller, simple controls/setups.

I. INTRODUCTION

THE proportional–integral (PI)-type controllers have proven to be remarkably effective and economical in regulating a wide range of processes in industry. It is inherently more robust and simpler than typical modern controllers that require an exact model. However, PI controllers generally suffer from the effect of integrator windup. This often leads to a large overshoot and a long settling time of the process output. To avoid this problem, many related methods have been reported under the names of conditional integration, limited integration, tracking antiwindup, and others [1]–[3]. Some of the antiwindup strategies only activate during saturation, and these provide limited improvement in performance. Others need an extra feedback compensation with some tuning parameters. The problem is “tuning” these parameters by selecting the proper values.

On the other hand, a commonly encountered control strategy for improving the performance of PI controller is to switch from

one control mode/gain to the other one. Industrial experience has shown that the P/PI speed control mode or gain switching is more effective in coping with the variety of different operating conditions for motion control [4]–[6]. In the P/PI mode switching method, integral action switches off (P control) when the control is far from the steady state and switches on (PI control) when the output is close to command [4]. In the speed control gain switching method, the integral gain increases when the motor speed is close to command and decreases in the transient state [5], [6]. The role of these methods may be considered almost the same since the integral action should be on or off to reduce the overshoot/undershoot of the speed responses.

A key question in the systems with P/PI control mode switching is how to find suitable switching variables and points. A few different switching variables are now used by industry servo drive manufacturer such as the torque command, the speed command/frequency, and the position error [4], [5]. It is necessary to have a good insight into the process dynamics to choose the adequate switching variables. To find the switching variables and switching points, therefore, the iterative manual tuning tests should be performed in the factory. Often, these iterative tests may cause mechanical and electrical problems in the field. Of course, this is far from an ease of use and simpler setup programming. In addition, the resulting speed responses at some given motion profiles are not consistent with other motion profiles. This process may appear to be an intimidating and time-consuming task. Despite the conceptual simplicity of conventional approaches, the practical implementation requires considerable efforts and time to obtain an acceptable response, which may translate into drive system downtime and loss of productivity.

The purpose of this paper is to describe our development of an automatic P/PI speed controller switching scheme for simple controls/setups. This scheme consequently improves the quality of motor dynamic characteristics. Analyzing the spectral content of the motor torque command in the frequency domain, the switching point of the P/PI controllers is automatically determined in real time. This greatly reduces the engineering effort for the machine builder since all codes are built-in to the amplifier. The dynamic performance of the proposed scheme assures a desired tracking response curve with minimal oscillation and settling time over all of the operating motion profiles. The proposed control scheme is applicable in conjunction with the existing cascaded control loop that is simple to implement in practice.

Manuscript received March 15, 2005.

J.-K. Seok and D.-C. Lee are with the School of Electrical Engineering, Yeungnam University, Kyongsan 712-749, Korea (e-mail: doljk@ynu.ac.kr).

K.-T. Kim is with the School of Electrical Engineering and Computer Science, Yeungnam University, Kyongsan 712-749, Korea (e-mail: juniorf@yumail.ac.kr).

Color versions of one or more of the figures in this paper are available online at <http://ieeexplore.ieee.org>.

Digital Object Identifier 10.1109/TIE.2007.899824

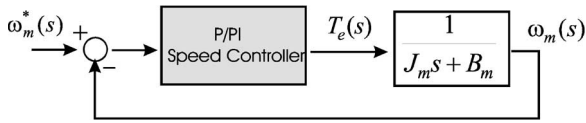


Fig. 1. Block diagram of the P/PI speed control system.

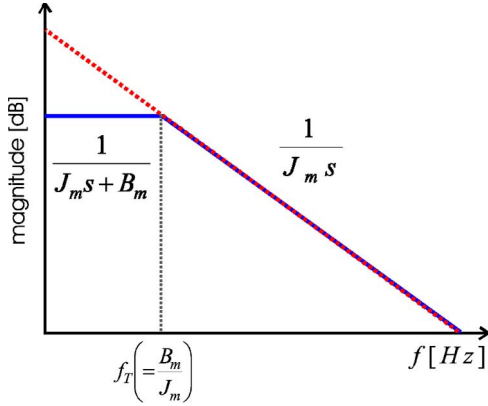


Fig. 2. Frequency response of the first-order mechanical system.

II. P/PI SPEED CONTROL MODE SWITCHING

For many processes in industry, servo applications can be controlled reasonably well by means of PI speed controllers. This is due to the fact that these processes can be described by means of a first-order model with a moment of inertia and viscous friction.

Fig. 1 shows the general block diagram of the speed control system where the speed command and speed feedback are represented by $\omega_m^*(s)$ and $\omega_m(s)$, respectively. The P/PI speed controller generates a motor torque $T_e(s)$ that tracks the torque command $T_e^*(s)$. The quantities J_m and B_m indicate the moment of inertia of the system and the viscous friction coefficient, respectively.

Fig. 2 shows the low-frequency and high-frequency characteristics of a first-order mechanical system. Above a break frequency f_T , the B_m term vanishes. This term is overwhelmed by the $J_m s$ term. Notice that well above f_T , the plot looks like $(1/J_m s)$: The magnitude falls with the frequency. For such a frequency range higher than f_T , there are no benefits with the PI controllers that may cause an overshoot and ringing due to an integral term of the speed error [7]. To guarantee a zero steady-state error, the speed controller should perform a PI control below f_T and switch to a P controller above f_T .

Based on the aforementioned concept, the conventional P/PI speed controller changes from a PI mode to a P mode if the switching variable under consideration exceeds the predefined setting value, and vice versa [4]–[6]. Fig. 3 shows an operating example of a conventional P/PI speed controller when the switching variable is selected as the torque command. In this case, the speed control loop successfully switches to P control in the high-frequency range. This leads to a fast response with a small overshoot or undershoot. In contrast, as shown in Fig. 4, the speed response has an overshoot/undershoot while the motor speed increases. This is due to the fact that the controller retains the same switching point as that of Fig. 3 and the switching from the PI mode to the P mode does not occur

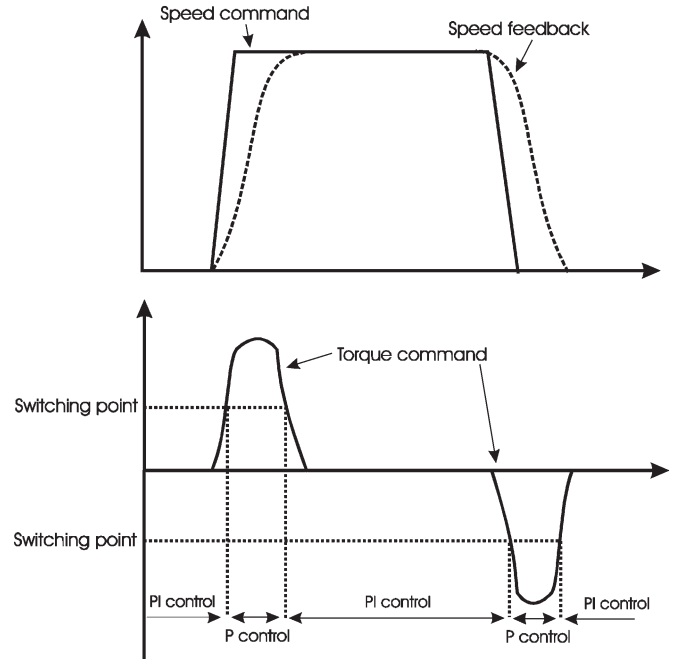


Fig. 3. Operating example of the conventional P/PI speed control scheme (I).

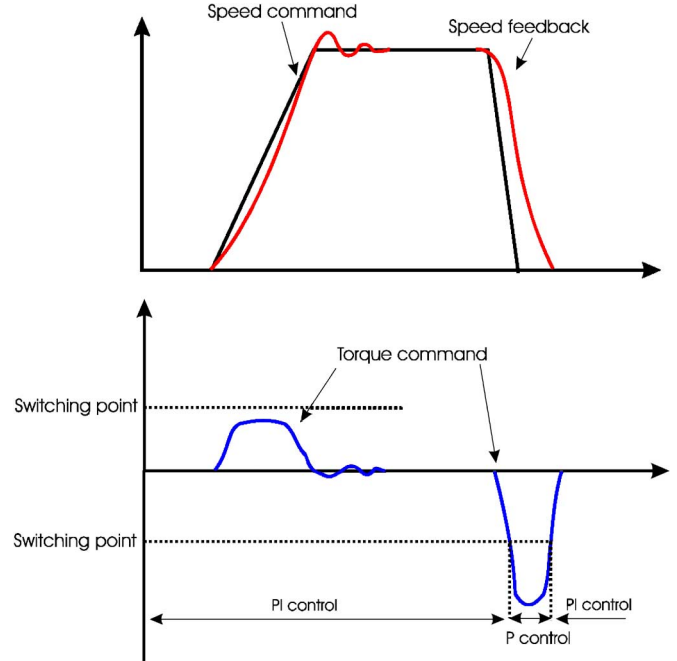


Fig. 4. Operating example of the conventional P/PI speed control scheme (II).

during acceleration. To prevent an undesirable speed response in this case, the switching points should be lowered according to the change of acceleration time.

Therefore, it can be concluded that the performance of a conventional P/PI controller with fixed switching points is heavily affected by the change of operating conditions such as the torque/speed command, the acceleration rate, load conditions, and controller gains. To satisfy the performance specification in all of the operating ranges, the switching point should be relocated according to the change of the operating condition. It can be quite a tedious job to find the best switching point, which may be undesirable in an industrial sense.

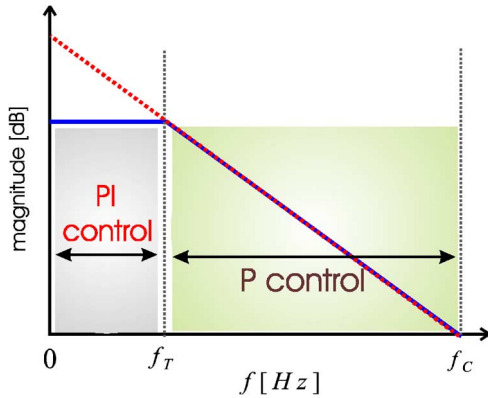


Fig. 5. Illustration of the P/PI speed controller switching in the frequency domain.

III. ONLINE SPECTRUM ANALYSIS

In practice, the speed sensor measurement is usually corrupted by measurement noise at low speeds. To avoid this problem, the output torque command is used as a tuning index signal in this paper. The torque command signal is an aperiodic discrete-time (DT) signal. The discrete Fourier transform (DFT) is used to analyze the torque command [8], [9]. The DFT is a mapping of an N sample torque command sequence $T_e^*[n]$ into another N sequence $X[k]$ in the frequency domain, i.e.,

$$X[k] = \sum_{n=0}^{N-1} T_e^*[n] e^{-j(2\pi/N)kn}, \quad k = 0, 1, 2, \dots, N-1 \quad (1)$$

where $X[k]$ is called the k th harmonics. This exists provided that all the samples of $T_e^*[n]$ are bounded. In this paper, we introduce the fast Fourier transform (FFT) to speed up the computation of the DFT coefficients. There have been many attempts to use the FFT in a variety of control applications. In [10] and [11], the frequency spectrum of various signals in a feedback system is computed using the FFT. These frequency spectra are fed back into the input to tune the process under control. In [12], the FFT has been exploited to estimate the rotational speed of the induction motor drives. An amplitude control of a vibration controller has been implemented by investigating the FFT spectrum of the vibration signal [13].

In terms of the quality of speed response, the PI controller is more favorable for $0 < f < f_T$ and the P controller for $f_T < f < f_C$. The parameter f_C is the crossover frequency that is uniquely determined by

$$\left| \frac{1}{J_m s} \right|_{s=j2\pi f_C} = 1. \quad (2)$$

The controller switching method in the frequency domain is illustrated in Fig. 5.

Generally, the discrete torque command signal exhibits a broad range of spectrum over time. This means that the signal can contain the unpredictable disturbances that can cause a variety of unreliable behavior with respect to the calculation of its spectrum level. To minimize the risk of online spectrum

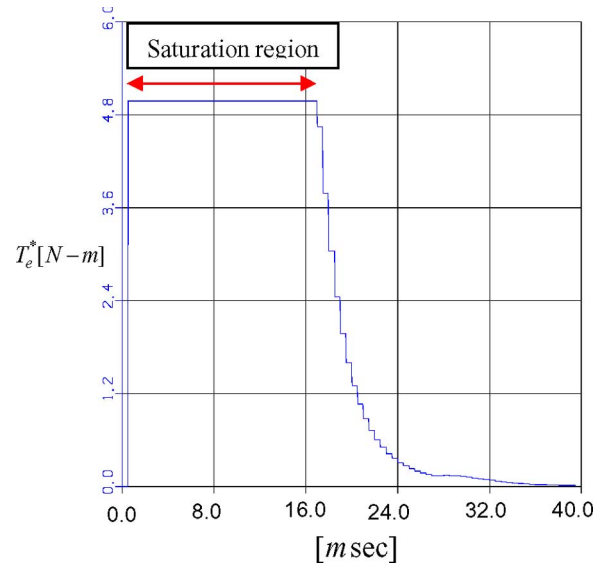


Fig. 6. Example of the torque command trajectory in the saturation region.

analysis penalized by noise or finite data set, an online spectral energy ratio R can be defined as

$$R = \frac{\sum_{k=N_T}^{N_C} |X[k]|^2}{\sum_{k=0}^{N_C} |X[k]|^2} \times 100[\%]. \quad (3)$$

In (3), the spectrum index is computed from

$$N_T = \text{int} \left(\frac{f_T}{f_s} N \right) \quad (4)$$

$$N_C = \text{int} \left(\frac{f_C}{f_s} N \right) \quad (5)$$

where f_s is a sampling frequency of the torque command.

In (3), the denominator represents the spectral energy that lies in the frequency band for $0 < f < f_s$ and the numerator for $0 < f < f_T$. This definition can be used directly to switch to the PI controller when the calculated spectral energy ratio is the condition of (6), and vice versa. Thus

$$R \leq 50[\%]. \quad (6)$$

IV. IMPLEMENTATION CONSIDERATIONS

A. Operation in the Saturation Region

Fig. 6 shows a typical torque command trajectory for the step speed command. The torque command increases initially because the speed error is positive. Then, the controller enters the saturation region, as shown in Fig. 6, resulting from the large value of the speed error. When this happens, the actual motor torque will remain at its limit independently of the controller output value. The motor torque limited by the saturation value contains the low-frequency content in the saturation region, but the controller output signal has the high-frequency content. This means that the spectral energy ratio of the actual output signal is larger than 50% and the integration should be suspended during saturation.

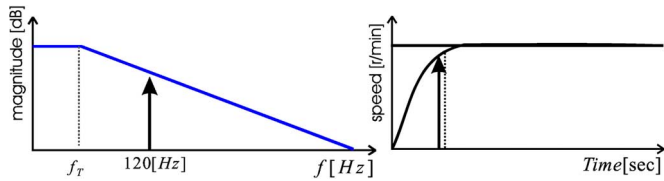


Fig. 7. Influence for the selection of the break frequency in the frequency and time domain.

B. Selection of Break Frequency

All commercial servo drives typically identify the mechanical inertia in an online and/or offline manner [4]–[6], but they do not involve the mechanical friction identification. Therefore, it is important that during an early stage of the controller design, a proper choice of f_T can be made with respect to a servo system with unknown mechanical friction.

When selecting f_T , in a practical point of view, two conditions are considered.

- 1) The minimum load inertia is the same as the motor inertia itself.
- 2) The maximum friction torque is less than 50% of the rated motor torque at rated speed.

Based on the aforementioned conditions, it is possible to obtain the information of break frequency of general servo motors on the market. Consequently, the maximum break frequency is not more than 55 Hz. By the simulation and experimental tests, we observe that the spectrum index in (4) should have a value of more than 2 to maintain enough resolution of the spectral energy ratio. In this paper, we set the break frequency to 120 Hz, which corresponds to $N_T = 3$ since the sampling frequency f_s and N are set to 5 kHz and 128, respectively. Hence, it is possible to determine the break frequency regardless of the friction uncertainties. This may result in an error for the selection of the correct break frequency in the frequency domain, but the error of the switching point in the time domain is relatively small, as shown in Fig. 7, such that the resulting performance is practically acceptable.

When the torque command has a high-frequency ripple around the selected break frequency, the proposed scheme could be affected by a limit cycle associated with an undesirable oscillation motion. However, this situation is rarely available in practice because the high-frequency torque ripple is not allowed in an actual servo system, which needs the high-precision torque control. In fact, all the commercial servo drives have a built-in digital low-pass filter to get rid of the high frequency of the torque command. Thus, it can be concluded that the performance of the proposed control scheme has little impact on limit cycles.

The proposed algorithm can also be applied to the integrator-windup-conscious industry applications that may frequently result in deep actuator saturation [14]. However, the operation of today's servo system with low inertia/torque ratio needs the shorter position-to-position movement, where the controller is not often driven into saturation. Thus, the antiwindup scheme is less effective in ensuring consistent control performance in the whole operating region. This can be explained by the fact that the today's commercial servo drives are still relying on the

TABLE I
RATINGS AND KNOWN PARAMETERS OF SERVO MOTOR UNDER TEST

Rating and Parameter	Value	Unit
Rated power output	400	W
Rated voltage	220	V
Rated speed	3000	r/min
Torque constant	0.332	Nm/A
Nominal motor inertia	3.6×10^{-5}	Kg-m ²
Viscous friction coefficient	1.8×10^{-4}	Nm/rad/s

embedded P/PI control mode switching algorithm to improve the speed response.

V. EXPERIMENTAL RESULTS

Extensive tests are performed to verify the proposed study. The algorithm is programmed and installed on a 400-W servo drive and motor, as indicated in Table I. The switching devices in the drive are insulated gate bipolar transistors with 10-kHz switching frequency. A TMS320VC33 digital signal processor is used as a main control processor, which operates at 120-MHz clock speed. The dc-link voltage is 300 V, and the sampling periods of the current and speed control are performed at every 50 and 200 μ s, respectively. The online FFT algorithm coded in assembly language is performed at every speed control period. The execution time is about 31 μ s for $N = 128$. The load inertia is coupled to the motor, and the inertia ratio is 5:1. The break frequency in the controller is set to 120 Hz. The PI gains of speed controller are given as follows:

$$\begin{aligned} K_p &= J_m \cdot \omega_{sp} \\ K_i &= K_p \cdot \omega_{sp} / 5. \end{aligned} \quad (7)$$

In all of the tests, the bandwidth of the speed controller ω_{sp} is set to 300 rad/s.

Fig. 8 shows the actual waveforms of the 500-r/min speed command for the conventional P/PI controller with the standard tracking antiwindup controller. From the top, the speed command/feedback, the torque command, and the switching flag are shown. The switching point is set to 80% of the rated torque by iterative tests at a given operating condition. The transient response is satisfactory, but this takes a lot of time adjusting the switching point.

Fig. 9 shows a typical problem when the conventional P/PI controller is adopted. The switching variable and point are the same as those in Fig. 8. Depending on PI controller gains, speed command profile, and mechanical system structure, the speed response may cause a severe instability problem in motion control systems. From “FlagKi,” it is observed that the mode switching to the P control does not occur. Therefore, it is seen that the conventional P/PI control mode switching is heavily affected by the operating conditions such as the speed command, the acceleration/deceleration rate, and load disturbances.

Fig. 10 shows the speed response of the proposed controller, where the running conditions are identical to those of Fig. 8. From the top, the spectral energy ratio, the speed feedback, the torque command, and the switching flag are depicted. The

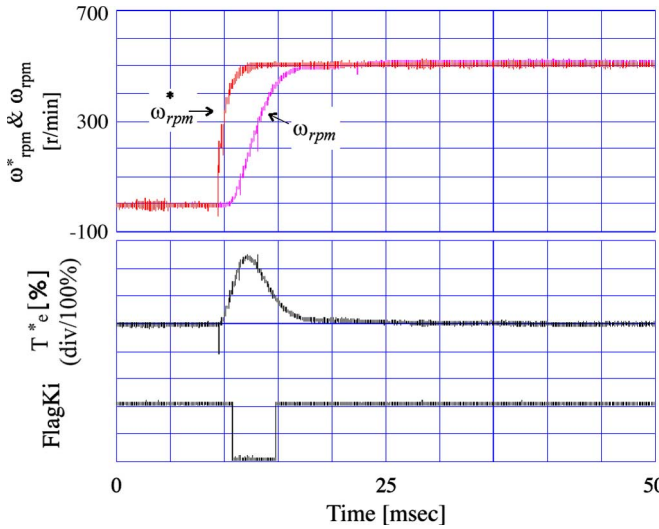


Fig. 8. Conventional P/PI switching scheme for the 500-r/min speed command.

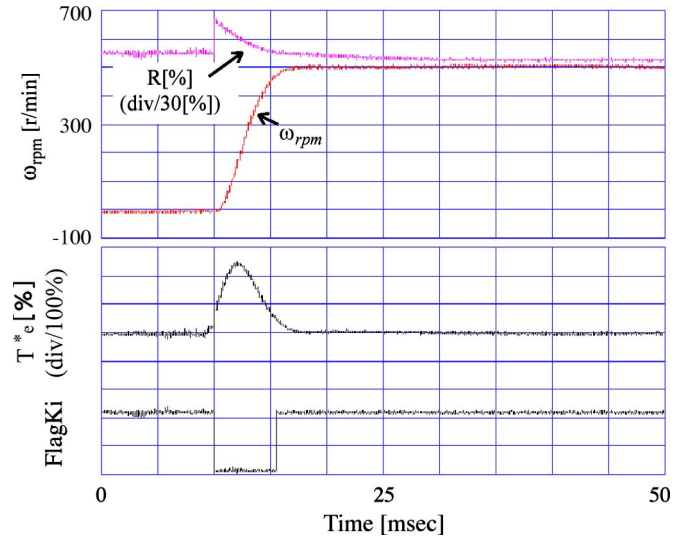


Fig. 10. Test results of the proposed scheme with the identical running condition of Fig. 8.

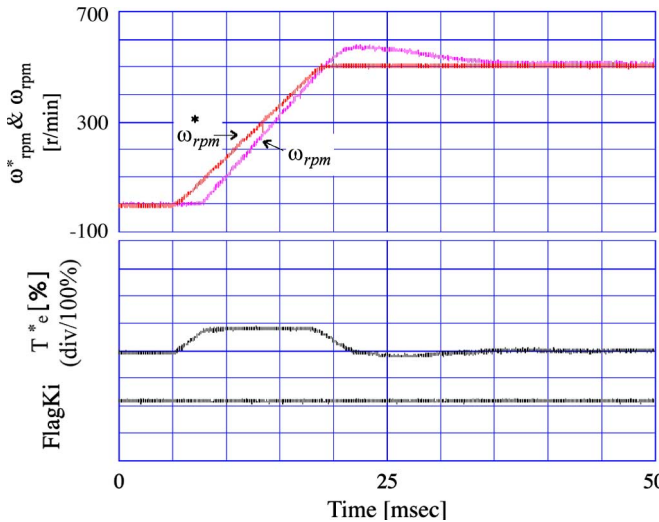


Fig. 9. Conventional P/PI switching scheme for the 500-r/min ramp speed command.

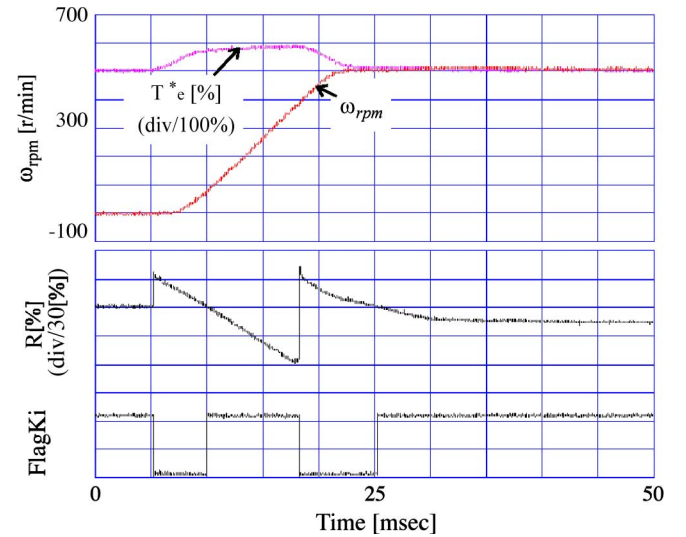


Fig. 11. Test results of the proposed scheme with the identical running condition of Fig. 9.

onset spectral energy ratio is set to 50%, and this scheme does not require any tuning tests prior to start-up. It can be noted that the P control mode duration is wider than that of Fig. 8. This difference means that the proposed control scheme determines the control mode using a different switching criterion.

Fig. 11 shows the comparison result with the identical running conditions of Fig. 9. From the top, the torque command, the speed feedback, the spectral energy ratio, and the switching flag are depicted. The control mode has automatically changed to P → PI → P mode according to the torque command spectrum energy. Employing the proposed control mode switching algorithm, the motor speed stays on a desired response curve for different operating conditions.

Fig. 12 shows the speed control performing under the condition that the speed command changes between 0 and 1000 r/min. From the top, the speed feedback, the spectral energy ratio, the switching flag, and the motor torque command

are shown. From this result, it is verified that the proposed method is very robust to operating condition changes.

Fig. 13 shows the 1000-r/min speed response with longer acceleration time than that of Fig. 12. According to the frequency content of the torque command signal, the control mode has automatically changed to P → PI → P mode. It is clear that the proposed scheme does not require iterative tunings in the field and is also helpful to an inexperienced user.

VI. CONCLUSION

Analyzing the spectral content of the motor torque command, the controller switching point is automatically determined, enabling the time-consuming experiments to be replaced by simple software calculations in the controller. After the proposed algorithm is installed, thereby, this gives a minimizing impact on product scheduling because iterative tunings for controller setup are one of the most critical factors delaying the commercial production on the line. The dynamic performance

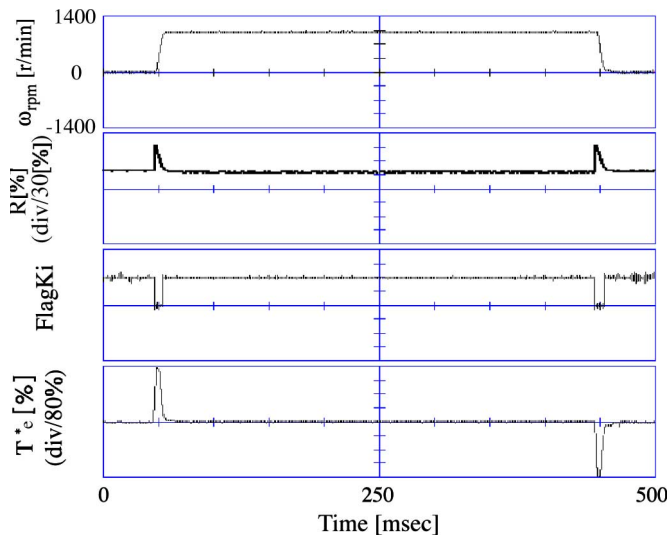


Fig. 12. Speed control performance with the proposed P/PI switching scheme for the 1000-r/min speed command.

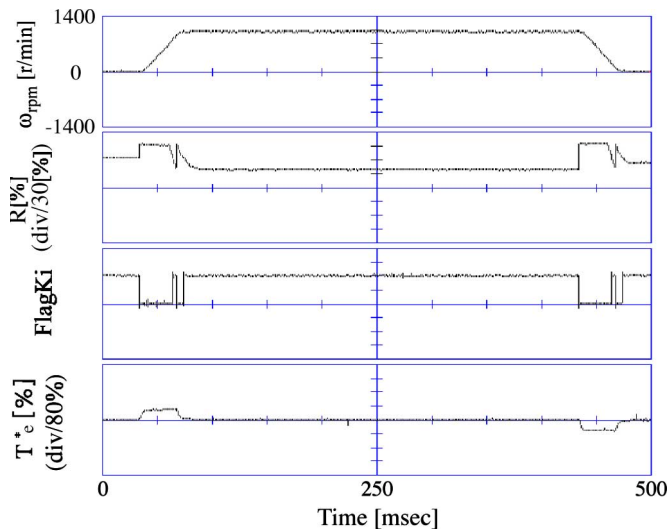


Fig. 13. Proposed P/PI switching scheme for the 1000-r/min speed command with the longer acceleration time.

of the proposed scheme assures a desired tracking response curve with minimal oscillation and settling time over the complete operating conditions. The proposed control scheme is also applicable in conjunction with the existing cascaded position control loop. For a comprehensive comparison of the conventional P/PI control scheme, extensive tests have been carried out on a 400-W servo drive system.

REFERENCES

- [1] C. Bohn and D. P. Atherton, "An analysis package comparing PID antiwindup strategies," *IEEE Control Syst. Mag.*, vol. 15, no. 2, pp. 34–40, Apr. 1995.
- [2] A. S. Hodel and E. C. E. Hall, "Variable-structure PID control to prevent integrator windup," *IEEE Trans. Ind. Electron.*, vol. 45, no. 3, pp. 445–450, Jun. 1998.
- [3] H. B. Shin, "New antiwindup PI controller for variable-speed motor drives," *IEEE Trans. Ind. Electron.*, vol. 48, no. 2, pp. 442–451, Apr. 1995.
- [4] *Sigma II Series Servo System User's Manual*, Yaskawa Electric Amer. Inc., Waukegan, IL, 2000.
- [5] *MELSERVO J2-Super Series Instruction Manual*, Mitsubishi Electric, Tokyo, Japan, 2001.

- [6] *Panasonic AC Servo Driver MINAS—A Series Operating Manual*, Matsushita Electric Ind. Company Ltd., Osaka, Japan, 2000.
- [7] K. J. Astrom and T. Hagglund, *PID Controllers: Theory, Design, and Tuning*. Research Triangle Park, NC: Instrum. Soc. Amer., 1995, pp. 120–200.
- [8] J. H. McClellan, R. W. Schafer, and M. A. Yoder, *DSP First: A Multimedia Approach*. Englewood Cliffs, NJ: Prentice-Hall, 1999, pp. 320–377.
- [9] D. G. Manolakis, V. K. Ingle, and S. M. Kogon, *Statistical and Adaptive Signal Processing*. New York: McGraw-Hill, 2000, pp. 195–225.
- [10] Q.-G. Wang, Q. Bi, and B. Zou, "Use of FFT in relay feedback systems," *Electron. Lett.*, vol. 33, no. 12, pp. 1099–1100, Jun. 1996.
- [11] J. J. Nelson, G. Venkataramanan, and A. M. EL-Refaie, "Fast thermal profiling of power semiconductor devices using Fourier techniques," *IEEE Trans. Ind. Electron.*, vol. 53, no. 2, pp. 521–529, Dec. 2006.
- [12] R. Blasco-Gimenez, G. M. Asher, M. Sumner, and K. J. Bradley, "Performance of FFT rotor slot harmonic speed detector for sensorless induction motor drives," *Proc. IEE—Elect. Power Appl.*, vol. 143, no. 3, pp. 258–268, May 1996.
- [13] N. Baoliang and Y. Xia, "A FFT-based variety sampling-rate sine sweep vibration controller," in *Proc. Neural Netw. and Signal Process. Conf.*, Dec. 2003, vol. 2, pp. 1714–1718.
- [14] J. K. Seok, "Frequency-spectrum-based antiwindup compensator for PI-controlled systems," *IEEE Trans. Ind. Electron.*, vol. 53, no. 6, pp. 1781–1790, Dec. 2006.



Jul-Ki Seok (S'94–M'98) received the B.S., M.S., and Ph.D. degrees from Seoul National University, Seoul, Korea, in 1992, 1994, and 1998, respectively, all in electrical engineering.

From 1998 to 2001, he was a Senior Engineer in the Production Engineering Center, Samsung Electronics, Suwon, Korea. Since 2001, he has been a member of the faculty of the School of Electrical Engineering, Yeungnam University, Kyongsan, Korea, where he is currently an Associate Professor. His specific research interests are in high-performance electrical machine drives, sensorless control of ac machines, and nonlinear system identification related to the power electronics field.



Kyung-Tae Kim received the B.S., M.S., and Ph.D. degrees in electronic engineering from the Pohang University of Science and Technology (POSTECH), Pohang, Korea, in 1994, 1996, and 1999, respectively.

During March 1999 to March 2001, he was with the Electromagnetics Technology Laboratory, POSTECH, as a Research Staff. During April 2001 to February 2002, he was a Research Assistant Professor in the Department of Electronic and Electrical Engineering, POSTECH. In March 2002, he joined the faculty of the School of Electrical Engineering and Computer Science, Yeungnam University, Kyongsan, Korea, where he is currently an Assistant Professor. His research interests include radar target identification, radar imaging, high-resolution spectral analysis, pattern recognition, neural networks, and RCS measurement and prediction.



Dong-Choon Lee (S'90–M'95) received the B.S., M.S., and Ph.D. degrees in electrical engineering from Seoul National University, Seoul, Korea, in 1985, 1987, and 1993, respectively.

He was a Research Engineer at Daewoo Heavy Industry from 1987 to 1988. He was with the Research Institute of Science Engineering, Seoul National University, under a postdoctoral fellowship for one year. Since 1994, he has been a member of the faculty of the Department of Electrical Engineering, Yeungnam University, Kyongsan, Korea. As a Visiting Scholar, he joined the Power Quality Laboratory, Texas A&M University, College Station, in 1998, the Electrical Drive Center, University of Nottingham, Nottingham, U.K., in 2001, and the Wisconsin Electric Machines and Power Electronic Consortium, University of Wisconsin, Madison, in 2004. His research interests include ac machine drives, control of power converters, wind power generation, and power quality.